Sensors & Actuators: B. Chemical 287 (2019) 390–397

Contents lists available at ScienceDirect

Sensors and Actuators B: Chemical

journal homepage: www.elsevier.com/locate/snb

Hydrodynamic-flow-enhanced rapid mixer for isothermal DNA hybridization kinetics analysis on digital microfluidics platform

Mingzhong Li[a,b], Cheng Dong[a], Man-Kay Law[a,*], Yanwei Jia[a,*], Pui-In Mak[a,b], Rui P. Martins[a,b,c]

[a] State Key Laboratory of Analog and Mixed-Signal VLSI, University of Macau, Macao, China
[b] Faculty of Science and Technology – Electrical and Computer Engineering, University of Macau, Macao, China
[c] On leave from Instituto Superior Técnico, Universidade de Lisboa, Lisboa, Portugal

ARTICLE INFO

Keywords:
DNA hybridization kinetics
Digital microfluidics
Hydrodynamic flow
Isothermal
Rapid mixing

ABSTRACT

DNA hybridization kinetics has been playing a critical role in molecular diagnostics for binding discrimination, but its study on digital microfluidic (DMF) systems is ultimately restrained by the laminar flow condition. The kinetic mixing technique is widely employed to ensure a fast reaction rate, but poses intrinsic risk in cross contamination and exhibits instable fluorescence intensity during the droplet transportation. While the electrothermal technique can provide stationary droplet mixing through the established thermal gradient within the hybridization solution, the significant increase in the droplet temperature will inevitably undermine the hybridization equilibrium and jeopardize the binding discrimination. To enhance the hybridization efficiency while ensuring a stable droplet temperature (within ± 0.1°C), this paper presents a DMF platform that can perform isothermal hydrodynamic-flow-enhanced droplet mixing. Specifically, with a single electrode, droplet-boundary oscillation under a slow AC actuation is studied for improving the reaction rate. The dependencies between the mixing efficiency and the actuation voltage, actuation frequency and the spacer thickness are also systematically studied. Reliable mixing efficiency improvement is further validated over a wide range of solute concentrations. The results from real-time on-chip DNA hybridization kinetics with stationary droplets using the complete sandwiched DMF system shows that the proposed rapid mixer can achieve the same hybridization equilibrium with > 13 times faster reaction rate when compared to the reference one through pure diffusion, while preventing biased hybridization kinetics as demonstrated in the electrothermal technique.

1. Introduction

DNA hybridization is a fundamental molecular interaction in biology research and medical applications, including gene identification, genetic expression analysis, DNA sequencing and clinical diagnostics [1–3]. This involves accurate and efficient DNA binding discrimination between the target and the probes with diverse concentrations at well-regulated temperatures [4,5]. Existing hybridization kinetics are mostly characterized in bulk solutions [1,6,7] under a high temperature accuracy requirement of ± 0.1 °C (e.g. Arrayit TrayMix™ S4 hybridization stations). To overcome the requirement of large amount of costly DNA samples, the electro-kinetic micro/nanofluidic technologies [8–10] offer many advantages including fast mixing/reaction rate, improved sensitivity, easy automation and real time monitoring. Even though the existing channel-microfluidic systems [11–14] are widely employed for DNA hybridization investigations, the redundant supporting equipment (valves, pumps or tubes) and risk of valve clogging still confine the system flexibilities for different diagnostic applications.

By manipulating micro-droplet via the electrowetting-on-dielectric (EWOD) effect, the DMF [15–18] offers high-level of controllability without the requirements of extra pumps and valves. It also presents additional flexibility for DNA probe immobilization for DNA hybridization kinetics [19,20]. However, one of the major hurdles to support real time DNA hybridization in DMF systems is the low Reynolds number, where the laminar flow condition as dominated by diffusion [21,22] ultimately limits the reaction rate and hence the system throughput. This calls for the development of efficient rapid micromixing techniques to achieve accurate and efficient hybridization under diverse medium concentration requirements.

As reported in [23–25], the kinetic mixing technique transports the coalesced droplet back and forth along a linear array of electrodes to enable the droplet mixing through the induced internal hydrodynamic flow. The mixing efficiency can be further enhanced using the 2-

* Corresponding authors at: University of Macau, Avenida da Universidade, Research Building N21, 3/F, Taipa, Macau, China.
E-mail addresses: mklaw@umac.mo (M.-K. Law), yanweijia@umac.mo (Y. Jia).

https://doi.org/10.1016/j.snb.2019.02.021
Received 18 September 2018; Received in revised form 17 January 2019; Accepted 5 February 2019
Available online 16 February 2019
0925-4005/

dimensional electrode-array by alleviating the flow reversibility effect. Many proposed DMF applications inevitably involve this kinetic mixing technique for sample pre-processing, dilution, and reactions between reagents [19,20,26–28]. Yet, the continuous transportation of biological samples can lead to nonspecific biomaterial adsorption [29] to the hydrophobic surface, increasing the risk of cross contamination and biofouling. Moreover, the varying instantaneous droplet velocity due to the frequent droplet displacement [30] can initiate unstable fluorescent intensities during the exposure period, which can undermine the study of on-chip real time DNA hybridization.

To enable rapid droplet mixing without introducing continuous droplet movement, a stationary droplet micro-mixing technique based on the electrothermal effect is reported [31]. By applying a fast-changing electric field beyond the Maxwell-Wagner interfacial relaxation frequency (f_{RC}) to the hybridization solution, the voltage drop across the dielectric membrane becomes negligible, resulting in the inability of adjusting the three-phase contact angle by varying the applied voltage. Instead, the induced inner temperature gradient ΔT can introduce internal electrothermal convection [32] to enhance the mixing and hybridization process. However, the mixing efficiency is highly dependent on the induced temperature gradient, which can significantly violate the DNA hybridization temperature requirement and possibly affect the DNA binding discrimination [33]. Besides, a significant ΔT is necessary for mixing efficiency improvement as the droplet concentration increases, making this technique unattractive to on-chip DNA hybridization.

In this paper, we introduce an integrated sandwiched DMF system capable of stationary DNA hybridization kinetics study as shown in Fig. 1. Rapid mixing of stationary droplet is proposed by using a slow AC actuation signal from 100 Hz to 1 kHz. Unlike [31] which is based on the electrothermal effect, this work takes advantage of the boundary oscillation condition of the coalesced droplet to achieve stationary mixing efficiency improvement through the enhanced internal hydrodynamic flow. The proposed technique is also applicable to medium at varying concentrations while maintaining a well-regulated droplet temperature due to a weak transient voltage drop across the droplet bulk, enabling fast on-chip real time DNA hybridization with minimal risk of cross contamination.

2. Materials and methods

2.1. Chemicals and reagents

The synthesized fluorophore DNA probe for Influenza A virus (H7N9) segment 4 hemagglutinin (HA) gene is from Integrated DNA Technologies (IDT, USA). The synthetic oligonucleotides (Sangon Biotech, China) used in the DNA hybridization kinetics experiments are DNA targets of *Kras* gene (drug resistant non-small cell lung cancer) and its corresponding molecular beacon (MB) probes with a stem of 1 base pair (BP). Below, we summarize the oligonucleotides employed in the experiments.

DNA probe for H7N9 DNA segment 4 HA:
5′-TTGACTTTCATTGGCTAATGCT-Cy3-3′.
DNA target of *Kras* gene:
5′-GTAGTTGGAGCTGGTGGCGTAGGCAAGAGT-3′.
MB probe for *Kras* gene target:
5′-Cy3-GCCTACGCCACCAGCTCC-BHQ2-3′.

The DNA probe for H7N9 DNA segment 4 HA, DNA target of *Kras* gene and its corresponding MB probe are dissolved and diluted to reach the final concentrations of 1, 5 and 10 μM using the 10 mM Tris − HCl buffer (Sigma, USA) with a conductivity of 1.52 mS/cm, a viscosity of 0.9307 mPa·s and a surface tension of 73 mN/m. The probe/target mixture for hybridization kinetics investigation is further formulated with 1 × PCR buffer (Life Technologies, USA), 3 mM $MgCl_2$ (Life Technologies, USA), and 1 μM MB probe/DNA target.

2.2. Device design and fabrication

Fig. 1(a) shows the DMF device under test with fabrication steps similar to our previous works [34]. Briefly, three different chromium (Cr) electrodes of 0.75 × 0.75, 1.5 × 1.5, and 2.5 × 2.5 mm^2 with 30 μm clearance from each other are designed for droplet

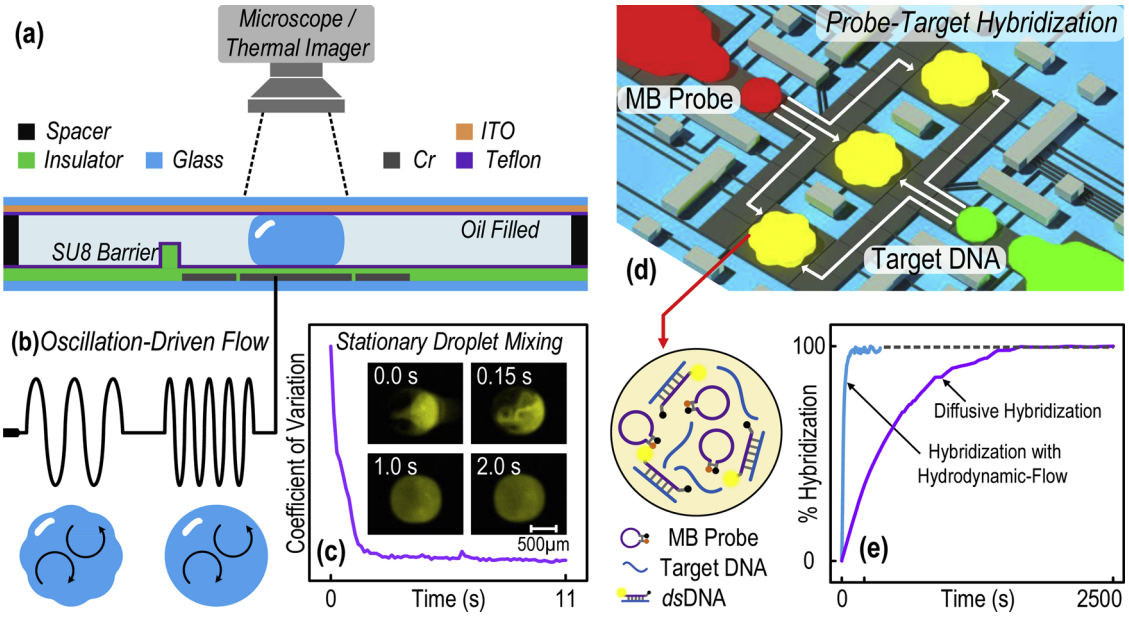

Fig. 1. (a) Schematic of the fabricated sandwiched DMF device with the reaction chamber monitored by a fluorescence microscope and thermal imager (not to scale). (b) Illustrations of the droplet oscillation patterns and internal hydrodynamic flow for mixing enhancement using a sub-kHz actuation frequency. (c) Characterization of the stationary droplet mixing with 1 μM fluorophore DNA probe and 10 mM Tris − HCl buffer. (d) Illustrative SE isometric view of the sandwiched DMF device for DNA hybridization kinetics study. The molecular beacon probe and target DNA are dispensed from the corresponding reservoirs and driven towards the reaction chambers. (e) Real-time DNA hybridization kinetics is observed through the fluorescence intensity for DNA binding with passive diffusion and the proposed hydrodynamic-flow enhancement method.

transportation, mixing, and dispensing, respectively. Different spacer thicknesses (150, 250, 350, 450 μm) are utilized to implement the sandwiched DMF platform with commercial conductive tapes, with the top plate (indium tin oxide glass) potential biased to ground. An insulation layer of 10 μm SU8 negative photoresist is deposited on the bottom plate to isolate the aqueous samples from the Cr electrodes to avoid unintentional electrochemical reactions. Patterned barriers using 50 μm thick SU8 negative photoresist through standard soft lithography are fabricated above the insulation layer to prevent droplets from drifting during the experiments. To increase the initial contact angles of the aqueous droplets and prevent sample adhesion, both the bottom substrate and the top plate are coated with a 100 nm thick hydrophobic Teflon-AF layer. The fabrication steps and chip assembly are detailed in the Supplementary Information S1.

2.3. Experimental setup

The DMF device is placed inside a 3D-printed device holder in all experiments. The fluorescence microscope and the thermal imager monitor the real-time mixing process and local droplet temperature status, respectively. All the DMF electronics are controlled by the customized software for droplet manipulation (e.g. sub-kHz actuation signal as shown in Fig. 1(b) for droplet vortexing). The detailed implementation of the hardware and software program can be found in the Supplementary Information S2 and S3. The DMF device under test together with the 3D-printed holder is mounted onto the stage of the fluorescence microscope (Olympus BX63, Japan). Real-time videos and images are recorded via the software cellSens©. The thermal imager (Fluke Ti110, USA) records the temperature variation inside the mixing droplet for further processing. The experimental setup is detailed in the Supplementary Information S4.

2.4. Video processing and data analysis

To quantitatively characterize the on-chip mixing efficiency, we assess the mixing conditions based on the pixels occupied by the entire coalesced droplet. The real-time videos, as recorded in the 24-bit Audio Video Interleaved (AVI) format, are processed by the customized software to extract the coefficient of variation (CV) of the j^{th} frame in the RGB colour space. Fig. 1(c) illustrates the mixing process between the 1 μM fluorophore DNA probe for H7N9 DNA segment 4 HA and 10 mM Tris−HCl buffer. The CV evolution is calculated using the corresponding RGB values as in Eqs. (1) and (2),

$$CV_j = (D_j - D_{min})/(D_{max} - D_{min}), \tag{1}$$

$$D_j = \frac{1}{N}\sum_{i=1}^{N}\sqrt{(R_i - \bar{R}_j)^2 + (G_i - \bar{G}_j)^2 + (B_i - \bar{B}_j)^2}, \tag{2}$$

where D is the average colour space distance between different colour components (i.e. R_i, G_i, B_i) of the i^{th} pixel to the current (j^{th}) frame average (i.e. $\bar{R}$, $\bar{G}$, $\bar{B}$), and N is the total number of occupied pixels of the coalesced droplet. The difference $(D_{max} - D_{min})$ denotes the full CV range for complete mixing with reference to the initial frame at time $t = 0$ where the CV is maximum (D_{max}). D_{min} is the average colour space distance in the steady state as dominated by random noise. A 5% CV threshold is enforced to indicate the droplet 95% mixing time (t_{95}).

2.5. Principle of stationary hydrodynamic-flow-enhanced micro-mixing

In this work, we propose a single-electrode stationary rapid micro-mixer using a slow AC actuation signal (below 1 kHz) to induce droplet boundary oscillation [35], which enhances the internal hydrodynamic flow as shown in Fig. 1(b). It can support rapid reagent mixing at well-regulated temperatures under a wide range of medium concentrations. According to the Young-Lippmann equation in (3), the droplet contact angle can be modulated between $\theta(t)$ and θ_0 with the AC electrowetting effect, which is due to the nonlinear electrical stress acting on the bipolar surface charge induced at the droplet and silicone oil interface, defined as

$$\cos\theta(t) = \cos\theta_0 + \frac{\varepsilon V(t)^2}{2\gamma d} = \cos\theta_0 + \frac{\varepsilon V_0^2(1 + cos(2\pi f_a t))}{4\gamma d} \tag{3}$$

where is the voltage drop across the dielectric membrane, γ is the liquid/filler media surface tension, and ε and d are the permittivity and thickness of the dielectric layer, respectively. Notice that the droplet contact angle defined in Eq. (3) can only be modulated with an actuation signal below f_{RC}. As is a time-varying component with an actuation frequency f_a, the three-phase contact line is periodically modulated between the spreading and the receding phase. Since $V(t)^2 = V_0^2 cos(2\pi f_a t)^2 = 0.5V_0^2 + 0.5V_0^2 cos(2 \times 2\pi f_a t)$, the oscillation component of the droplet is at twice the actuation frequency (i.e. $f = 2f_a$), which is consistent with previous observations [36] using open DMF platforms.

This oscillation can directly lead to the pressure adjustment at the droplet boundary, leading to boundary deformation. As discussed in [35], the pressure within the droplet is also proportional to $V(t)^2$ with an oscillation frequency of $2f_a$. The centre of mass of the droplet fluctuates due to both the boundary oscillation and the corresponding pressure modulation mechanisms, which further lead to the droplet internal hydrodynamic flow (i.e. drift of the fluid [35]). Such effect can greatly enhance the molecular collisions and therefore the corresponding mixing efficiency in the sandwiched droplets, as shown in Fig. 1(b, c).

Benefit from this mechanical mixing enhancement technique, well-regulated temperatures in the droplet can be achieved. The displacement current across the dielectric membrane can also be greatly inhibited due to the low actuation frequencies (in the range of kHz). This limits the ohmic current flowing through the conductive droplet to be at the nano-/pico-Ampere level, contributing negligible power dissipations on the droplet.

2.6. DMF procedure for DNA hybridization kinetics investigation

Fig. 1(d) shows the overview of the DMF device for the investigation of DNA hybridization kinetics with the proposed rapid micro-mixing technique. Both flanks with reservoirs serve to dispense and transport the MB probe and the target DNA to the middle chambers for stationary rapid mixing/hybridization in oil phase (silicone oil, 1 cSt, Clearco, USA). A large mixing chamber is utilized to accommodate for the droplet deformation during the experiments so as to maintain a uniform global electric field across the entire droplet for mixing/hybridization efficiency evaluation. To initialize the hybridization process, we applied an AC sinusoidal waveform ranging from 100 Hz to 1k Hz to the chambers. The fluorescence intensity and temperature fluctuation of the hybridization process are recorded in real-time as illustrated in Fig. 1(e). The chambers are kept activated throughout the experiment to ensure a steady mixing environment.

3. Results and discussion

3.1. Driving frequency

Here we study the effect of the driving frequency on the droplet mixing efficiency in the proposed DMF platform. Two droplets containing 1 μM DNA (DNA probe for H7N9 DNA segment 4 HA), and 10 mM Tris−HCl buffer are dispensed and mixed together. The fluorescence intensity change of the coalesced droplet is used to evaluate the mixture homogeneity. A wide actuation frequency ranging from 100 Hz to 10 kHz with a voltage amplitude of 150 V_{rms} is applied to the coalesced droplet for rapid micro-mixing. For higher frequencies above 10 kHz up to 6 MHz, the applied voltage is set to 100 V_{rms} due to the

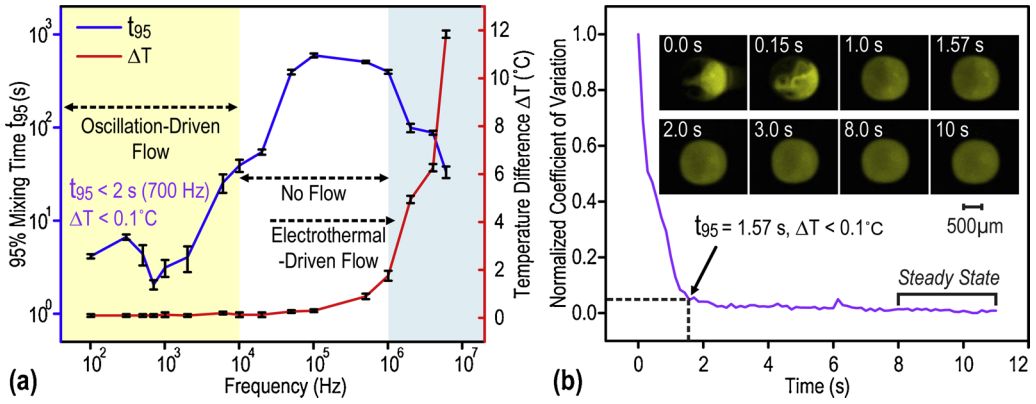

Fig. 2. (a) The effect of frequency on the mixing efficiency and temperature variation of the mixing droplet, consisting of 1 μM DNA and 10 mM Tris – HCl buffer with a diameter of approximately 800 μm at 150 μm spacer thickness. The amplitude of the applied voltage is set @ 150 V_{rms} (100 Hz – 10 kHz) and 100 V_{rms} (20 kHz – 6 MHz). We have conducted 3 independent experiments at ambient temperature (25 °C), showing that a sub-kHz actuation frequency can improve the mixing time without increasing the droplet temperature. (b) Example mixing process with experimental images at 150 V_{rms} (700 Hz) and 150 μm spacer thickness, showing a 95% mixing time of < 2 s based on the normalized coefficient of variation (CV). See Supplementary Video Information SV1.

limitation of the test setup. Theoretically, as the frequency gradually increases beyond f_{RC}, the magnitude of the boundary oscillation diminishes which is consistent with [36]. The temperature variation of the coalesced droplet is real-time monitored to characterize its relationship with the applied driving frequency. We control the droplet size to have a diameter of approximately 800 μm. The spacer thickness is fixed at 150 μm. Fig. 2(a) shows the measured 95% mixing time t_{95} with respect to the actuation frequency. At a fixed driving voltage of 150 V_{rms}, we observe internal hydrodynamic flow induced by the droplet boundary oscillation from 100 Hz to 10 kHz. From Fig. 2(a), we can observe that the droplet temperature change is within ± 0.1 °C (limited by the thermal imager accuracy), as there is no observable electric-field gradient found across the droplet in the low frequency range [37]. As the frequency further increases, a weak electric-field gradient is established, causing an increase in the droplet temperature. During the experiment, the no-flow state is detected within the 10 kHz and 1 MHz range, where the mixing process is dominated by pure diffusion with a much longer mixing time of > 50 s. When the frequency is beyond 1 MHz, internal flow inside the droplet reappears due to the electrothermal effect [38–41]. The significant electric field induces local elevated temperature gradient ΔT, which in turn varies the permittivity and conductivity inside the droplet in the microscopic scale to improve the mixing efficiency. With a 150 μm spacer thickness, the minimum mixing time for the homogenous DNA mixing experiments are 2.03 s at 700 Hz (150 V_{rms}, ΔT < 0.1°C) and 33.38 s at 6 MHz (100 V_{rms}, ΔT = 11.9 °C), respectively. Fig. 2(b) shows the normalized CV at 700 Hz, with the evolution of the mixing conditions illustrated in the image insets. The mixing efficiency improvement as observed is important for the development of biochemical applications on DMF platforms. For selective synthesis [42–44] targeting high product yield and purity, efficient mixing of original reactants can promote the primary reactions and suppresses the undesired consecutive side reactions. Apart from that, reaction kinetics characterization can be another important scenario for reaction quantification and assessment, since the reaction rate can vary significantly due to the reaction chamber configuration and the homogeneity of the mixed reactants. Efficient mixing is a major bottleneck on DMF platforms due to the intrinsic laminar flow conditions, and it ultimately restrains the development of on-chip DNA hybridization and high throughput molecular diagnostics.

Even though we cannot perform experiments at a frequency of > 6 MHz due to the test setup limitation, the trend to further shorten the mixing time at a higher mixing frequency can still be anticipated. However, as observed in Fig. 2(a), the droplet temperature can also increase exponentially as frequency increases due to the augmented droplet power dissipation P_L . With negligible ITO resistance, P_L can be defined in Eq. (4), as

$$P_L = V_L \times I_L = \frac{V_L^2}{R_L} \approx R_L \times \left(\frac{V_{rms}}{R_L + \frac{1}{2\pi f_a C_D}}\right)^2, \; with \; R_L \ll X_L \tag{4}$$

where V_{rms} is the root-mean-square value of the actuation AC signal, V_L and I_L are the voltage drop and ohmic current across over the droplet, f_a is the actuation frequency, R_L are the resistance of the conductive droplet, C_D is the capacitance of the dielectric membrane, and X_L and X_D are the reactance of the sandwiched droplet and dielectric membrane, respectively. At high actuation frequencies, the droplet voltage increases, leading to a higher power dissipation across the droplet and hence an increased temperature, which is consistent with observation and measurement.

The electrothermal effect becomes significant when the frequency is > 1 MHz, also shown in Fig. 2(a). Though the temperature increase within the droplet using high frequencies can be beneficial to some biochemical assays which require fast local temperature modulation, the increased current flow and weak temperature control within the mixing droplets can conversely impair the experimental conditions for temperature sensitive assays including DNA hybridization, drug screening and living cell cultivation [45,46]. As an example, the elevated temperature can reduce the enzyme activity and even cause the enzyme to denature, which will inevitably undermine the DNA hybridization efficiency and damage the rate of cell metabolism in PCR and cell experiments. Based on our results, an actuation frequency from 100 Hz to 1 kHz, which is best suited for the investigation of hybridization kinetics, is selected for the subsequent experiments.

3.2. Voltage amplitude and device spacer thickness

Besides the actuation frequency, the driving voltage amplitude as well as the spacer thickness also play key roles in affecting the mixing efficiency. Their influences are investigated by using the identical experimental settings as mentioned above, i.e. 1 μM DNA (DNA probe for H7N9 DNA segment 4 HA) and 10 mM Tris – HCl buffer. Fig. 3(a) shows the experimental results using 75, 100, 150, and 200 V_{rms} with a spacer thickness of 150 μm. Though the initiation of the boundary oscillation and internal hydrodynamic flow is independent of the applied voltage amplitude, the oscillation and flow magnitudes become stronger as the voltage amplitude increases. Despite achieving a fastest mixing time of 1.63 s at 200 V_{rms} (700 Hz), the contact line of the coalesced droplet becomes extremely unstable and the ejected pico-litre satellite droplets can undermine the target solution concentration. Consequently, we select a driving voltage amplitude of 150 V_{rms}, which exhibits comparable mixing speed, for the subsequent experiments.

Fig. 3(b) shows the mixing performance with four different spacer thickness: 150, 250, 350, and 450 μm at 150 V_{rms}. For each case, we maintain the droplet size to have a diameter of approximately 800 μm for both the initial droplets. The experimental results show that the

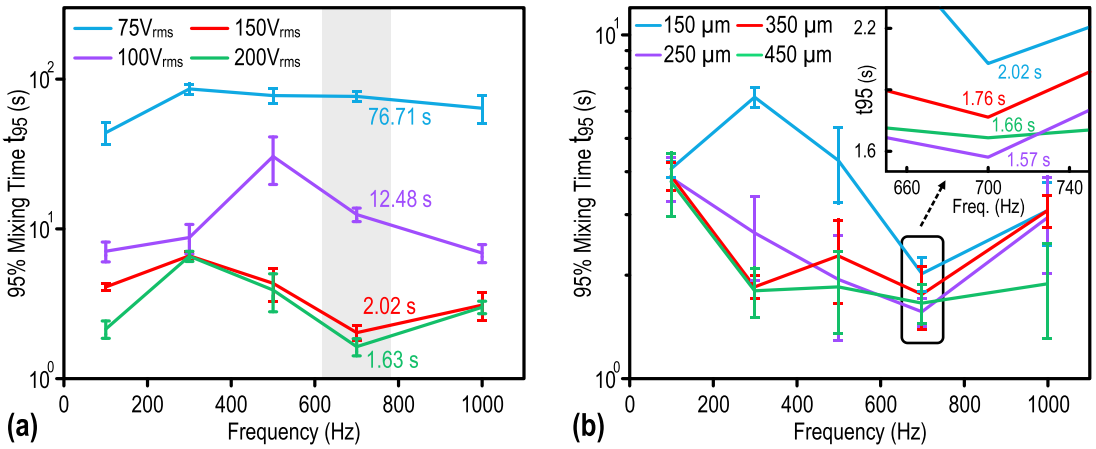

Fig. 3. Experimental results illustrating the 95% mixing time versus the driving frequency from 100 Hz to 1000 Hz at (a) different actuation voltages with a 150 μm spacer thickness configuration; and (b) different spacer thicknesses @ 150 V_{rms}. We have performed 3 trials with constant droplet size (diameters of approximately 800 μm) at ambient temperature (25 °C). The general trend of a faster mixing time with either a higher actuation voltage or a larger spacer thickness can be observed.

spacer thickness can affect the droplet mixing efficiency, and the fastest mixing time is 1.57 s with a spacer thickness of > 250 μm (150 V_{rms}, 700 Hz). This is due to the enhancement of the vertical fluid flow as the gap height increases. However, this is also a direct trade-off with the electric field strength across the droplet under the same driving voltage amplitude (and hence the droplet boundary oscillation amplitude). Apart from that, a wider spacer thickness can also jeopardize normal DMF functions such as droplet splitting and dispensing. Consequently, a spacer thickness of 150 μm is selected as it provides a comparable mixing performance while supporting all the droplet manipulation functions.

3.3. DNA concentrations in Tris – HCl buffer

Rapid mixing of diverse solute concentrations is necessary for flexible DNA hybridization kinetics investigations. Here, we investigate the impact of DNA molecules at different reagent concentrations on the mixing efficiency. Fig. 4(a) presents the mixing time using diverse DNA molecule concentrations (1, 5, and 10 μM) of DNA probe for H7N9 DNA segment 4 HA in a 10 mM Tris – HCl buffer. In theory, a higher molecule concentration can increase the solution viscosity and consequently enhance the shear force $\boldsymbol{F_s}$ as defined in Eq. (5),

$$\boldsymbol{F_s} = (2\pi \boldsymbol{r}^2) \cdot \frac{6\eta \mathcal{V}}{\boldsymbol{h}} \tag{5}$$

where $\boldsymbol{h}$ is the spacer thickness, and $\boldsymbol{r}$, η, and $\mathcal{V}$ are the radius, viscosity, and velocity of the droplet, respectively. This shear force should oppose the diffusive mixing process and increase the mixing time. However, as observed in Fig. 4(b), the measured normalized CV evolution with respect to the mixing time using 1, 5, and 10 μM DNA are 2.02 s, 1.37 s, and 1.28 s under 150 V_{rms} (700 Hz), respectively. The negative correlation between the experimental mixing time and the DNA concentrations regardless of the applied actuation frequency can be resulted from the rapid dispersion of the DNA molecules in the presence of the hydrodynamic flow. This can mitigate the shear force effect and enhance the molecular diffusion within the mixing droplet. One interesting observation is that unlike the electrothermal technique [31] where the required inner temperature gradient for active mixing is highly dependent on the reagent concentrations, our proposed technique can achieve consistent mixing time reduction throughout the experiments. This can further support the mixing-sensitive bioanalysis, such as hybridization kinetics investigation with wide-range solute concentrations. Apart from that, the possibility of rapid mixing independent of medium concentrations can also alleviate the non-specific reactions (e.g. competitive-consecutive and competitive-parallel types) in the chemosynthesis and synthesis of nucleic acid, leading to the reduction of undesired by-products and increase in the product stability.

3.4. DNA hybridization kinetics on DMF

Accurate and efficient hybridization kinetics plays a critical role in molecular diagnostics to discriminate the perfectly matched DNA binding over the mismatched one for cancer subtypes classification, pathogen and polymorphisms identification, etc. We demonstrate the suitability of our proposed technique for the investigation of on-chip real-time DNA hybridization kinetics using the DNA target of *Kras* gene and its corresponding hairpin structured molecular beacon probes. The length of the stem in the molecular beacon probe is 1 base pair (bp)

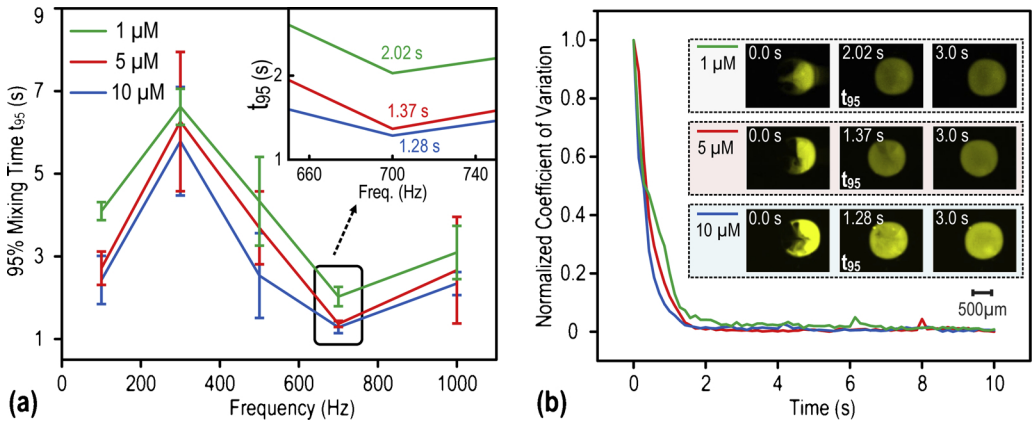

Fig. 4. Experimental results illustrating the 95% mixing time versus the driving frequency from 100 Hz to 1000 Hz at 150 V_{rms} in 150 μm spacer thickness configuration: (a) DNA (1 μM, 5 μM, and 10 μM) with 10 mM Tris – HCl buffer. (b) Normalized CV with experimental mixing images for 1, 5, and 10 μM DNA dilution with 10 mM Tris – HCl buffer at 150 V_{rms} (700 Hz). We have conducted 3 trials for each experiment at ambient temperature (25 °C), showing a faster mixing time at higher molecule concentrations.

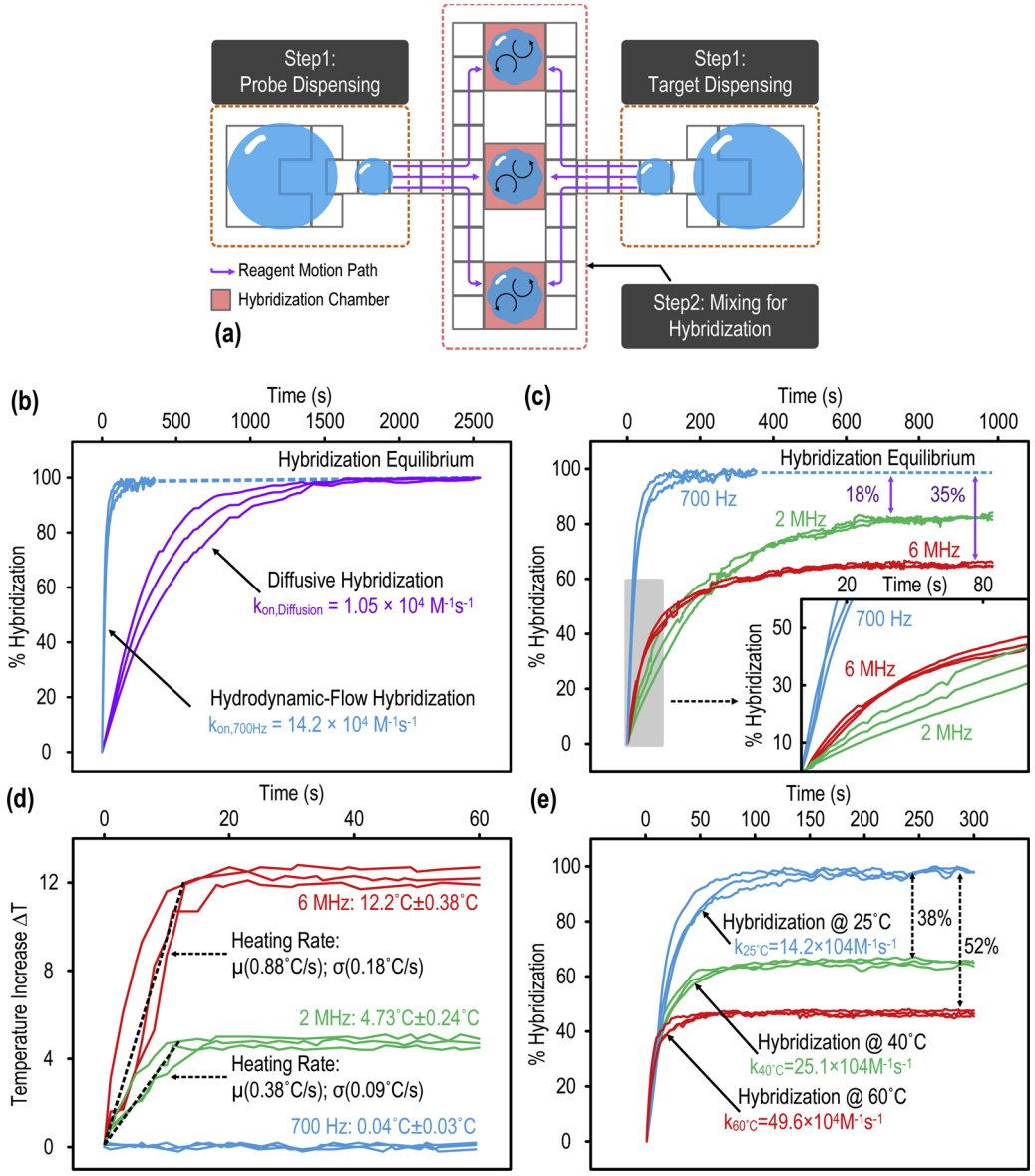

Fig. 5. Hybridization kinetics of the molecular beacons in the presence of 1 μM DNA target of *Kras* gene related to lung cancer. (a) DMF device for the investigation of target-beacon hybridization kinetics. The DNA hybridization process are performed at 25 ℃ and 150 μm configuration with three trials each: (b) pure diffusion and 700 Hz mixing at 150 Vrms; and (c) 700 Hz mixing at 150 V_{rms} and 2 MHz and 6 MHz at 100 V_{rms}. The hybridization reaction in 700 Hz achieves the faster hybridization equilibrium and on-rate constant ($k_{on,\ 700Hz} = 14.2 \times 10^4 M^{-1}s^{-1}$) than the diffusion one ($k_{on,\ diffusion} = 1.05 \times 10^4 M^{-1}s^{-1}$). Biased hybridization kinetics are observed with 2 and 6 MHz driving frequencies, which elevate the temperature in the hybridization solutions as illustrated in (d). Hybridizations conducted at 25 ˚C, 40 ˚C and 60 ˚C, with $k_{40\circ C} = 25.1 \times 10^4 M^{-1}s^{-1}$ and $k_{60\circ C} = 49.6 \times 10^4 M^{-1}s^{-1}$, as shown in (e). See Supplementary Video Information SV2.

while the loop structure is 16 bases. The melting temperature (Tm) of the hybrid double strand DNA (*ds*DNA) is 73.5 ℃. All the molecular beacon probes are labelled with the identical Cy3 fluorophore at one end and a BHQ2 quencher at the other. We observe the hybridization kinetics through the real-time monitoring of the fluorescence intensity. We have also compared with the existing stationary mixing method, i.e. the electrothermal technique in [31], using the same experimental setup.

The DNA hybridization assays are conducted at ambient temperature of 25 ℃ to ensure enough probe-target binding. As shown in Fig. 5(a), 1 μM of the DNA target and the molecular beacon probe are dispensed and transported to the reaction chambers for continuous fluorescence monitoring of the hybridization solution. Fig. 5(b, c) illustrates the fluorescence restoration in percentage as a function of time under different experimental conditions. As observed in Fig. 5(b), the efficiency of hybridization kinetics under pure diffusion is 13.52× slower than the proposed technique using a 700-Hz actuation for reaching the hybridization equilibrium. The corresponding reaction on-rate constants are $k_{on,\ diffusion} = 1.05 \times 10^4 M^{-1}s^{-1}$ and $k_{on,\ 700Hz} = 14.2 \times 10^4 M^{-1}s^{-1}$, respectively. However, even with the perfectly matched targets and probes, biased hybridization kinetics in the form of mismatched DNA binding is observed using the electrothermal technique with 2 MHz and 6 MHz driving frequencies, where the hybridization equilibrium are 18% and 35% lower than the reference (i.e. based on pure diffusion), respectively. This is mainly caused by the elevated temperature inside the DNA binding droplet ($\Delta T_{equil,\ 2MHz} = 4.73˚C$, and $\Delta T_{equil,\ 6MHz} = 12.2˚C$) due to the excessive power dissipated as explained in Eq. (4). Fig. 5(d) compares the droplet temperature variation using the proposed technique @ 700 Hz actuation and the electrothermal effect @ 2 MHz and 6 MHz. It can be observed that the temperature in the hybridization solution based on the electrothermal technique keeps increasing before reaching the

equilibrium, showing a heating rate of 0.38 and 0.88 ℃/s, respectively. However, the proposed technique exhibits negligible droplet temperature change of within ± 0.1 ℃. The final amount of the hybrid *ds*DNA can also accurately yet rapidly approach to the reference hybridization equilibrium based on pure diffusion, as observed in Fig. 5(b), demonstrating the proposed technique as a promising method for future temperature and mixing sensitive applications.

Detection sensitivity of the fluorescence intensity can be an important parameter for quantifying the DNA target molecules. As shown in Fig. 5(c), hybridization at 700-Hz can achieve 2.4× and 3.9× higher detection sensitivity at a reaction/testing time of 60 s when compared to the 2-MHz and 6-MHz ones, respectively. This is mainly due to the elevated droplet temperature at high mixing frequencies. Since the hybridization in this work is a single chemical reaction without any competitive-consecutive schemes, the measured final quantities of the hybridized *ds*DNA between the hybridization at 700-Hz and the diffusive one should be identical, as shown in Fig. 5(b). Due to the non-homogenous environment, the reaction time of DNA hybridization characterization in DMF platforms using pure diffusion can be especially long (in the order of few to tens of minutes), which can significantly limit the throughput of the DMF system. The proposed mixing technique can resolve this issue and result in a 13.52× improvement in reaction rate, as well as a 6.9× higher detection sensitivity at a reaction/testing time of 60 s when compare with the pure diffusive one.

Apart from characterizing the DNA hybridizations at room temperature (i.e. 25 ˚C), we have also conducted identical experiments at 40 ˚C and 60 ˚C for investigating the temperature effect on the hybridization efficiency. As illustrated in Fig. 5(e), with the proposed mixing technique at 700-Hz, the hybridization kinetics at 25 ˚C can be calculated to be 1.77×, and 3.49× slower than those at 40 ˚C and 60 ˚C, respectively. This can be due to the enhanced molecular kinetic energy at increased operating temperature. The corresponding on-rate constants under each operating temperature are $k_{25°C} = 14.2 \times 10^4 M^{-1}s^{-1}$, $k_{40°C} = 25.1 \times 10^4 M^{-1}s^{-1}$, and $k_{60°C} = 49.6 \times 10^4 M^{-1}s^{-1}$, respectively. However, the fluorescence equilibrium is 38%, and 52% higher for the 25 ˚C case, indicating that lower DNA hybridization efficiency and undermined detection sensitivity take place at higher temperature conditions. As observed, DNA hybridization at higher temperature not only comes with enhanced hybridization kinetics but also reaches the fluorescence equilibrium faster.

4. Conclusions

This paper describes a novel in-situ mixing enhancement technique that mitigates the prominent cross-contamination issue in conventional kinetic mixing methods, enabling the development of high-throughput yet accurate hybridization kinetics on DMF systems. Comprehensive investigations have been carried out to evaluate the mixing performance in terms of the actuation frequency, voltage amplitude, and spacer thickness. With the droplet boundary oscillation induced internal hydrodynamic flow, the optimal actuation frequencies for rapid mixing under different experimental settings are found in the range from 100 Hz to 1k Hz. Benefitting from the mechanical mixing process, the proposed method can achieve efficient mixing independently of the solute concentrations for flexible hybridization experiments. The negligible temperature change is also favourable for the discrimination of matched and mismatched binding for the DNA hybridization kinetics investigation. Based on the hybridization experiments of *Kras* gene and its corresponding molecular beacon probe in a complete DMF platform, the hybridization equilibrium is more readily and accurately achieved with the proposed micro-mixing technique over the diffusion and the electrothermal counterparts on DMF platform. This rapid, homogeneous, and temperature-stable mixing technique is also envisioned to provide opportunities for practical applications in chemosynthesis, bioanalysis, drug delivery, and synthesis of nucleic acid on DMF systems.

Conflicts of interest

There are no conflicts of interest to declare.

Acknowledgements

The authors would like to thank Dr. Tianlan Chen, Ms. Liang Wan and Dr. Jie Gao for the valuable discussions, as well as Macao FDCT – SKL fund and the research committee of the University of Macau (MYRG2017-AMSV-00221) for financial support.

Appendix A. Supplementary data

Supplementary material related to this article can be found, in the online version, at doi:https://doi.org/10.1016/j.snb.2019.02.021.

References

[1] Y. Jia, J.A. Sanchez, L.J. Wangh, Kinetic hairpin oligonucleotide blockers for selective amplification of rare mutations, Sci. Rep. 4 (2014) 5921.
[2] M.B. Clark, T.R. Mercer, G. Bussotti, T. Leonardi, K.R. Haynes, J. Crawford, M.E. Brunck, K.-A.L. Cao, G.P. Thomas, W.Y. Chen, R.J. Taft, L.K. Nielsen, A.J. Enright, J.S. Mattick, M.E. Dinger, Quantitative gene profiling of long non-coding RNAs with targeted RNA sequencing, Nat. Methods 12 (2015) 339–342.
[3] J.X. Zhang, J.Z. Fang, W. Duan, L.R. Wu, A.W. Zhang, N. Dalchau, B. Yordanov, R. Petersen, A. Phillips, D.Y. Zhang, Predicting DNA hybridization kinetics from sequence, Nat. Chem. 10 (2017) 91–98.
[4] N.V. Sorokin, V.R. Chechetkin, M.A. Livshits, S.V. Pan'kov, M.Y. Donnikov, D.A. Gryadunov, S.A. Lapa, A.S. Zasedatelev, Discrimination between perfect and mismatched duplexes with oligonucleotide gel microchips: role of thermodynamic and kinetic effects during hybridization, J. Biomol. Struct. Dyn. 22 (2005) 725–734.
[5] P. Sykacek, D.P. Kreil, L.A. Meadows, R.P. Auburn, B. Fischer, S. Russell, G. Micklem, The impact of quantitative optimization of hybridization conditions on gene expression analysis, BMC Bioinformatics 12 (2011) 73.
[6] J.S. Schreck, T.E. Ouldridge, F. Romano, P. Šulc, L.P. Shaw, A.A. Louis, J.P.K. Doye, DNA hairpins destabilize duplexes primarily by promoting melting rather than by inhibiting hybridization, Nucleic Acids Res. 43 (2015) 6181–6190.
[7] Y. Okahata, M. Kawase, K. Niikura, F. Ohtake, H. Furusawa, Y. Ebara, Kinetic measurements of DNA hybridization on an oligonucleotide-immobilized 27-MHz quartz crystal microbalance, Anal. Chem. 70 (1998) 1288–1296.
[8] W. Liu, Y. Ren, Y. Tao, B. Yao, N. Liu, Q. Wu, A universal design of field-effect-tunable microfluidic ion diode based on a gating cation-exchange nanoporous membrane, Phys. Fluids 29 (2017) 112001.
[9] W. Liu, Y. Ren, Y. Tao, X. Chen, B. Yao, M. Hui, L. Bai, Control of two-phase flow in microfluidics using out-of-phase electroconvective streaming, Phys. Fluids 29 (2017) 112002.
[10] Y. Ren, C. Song, W. Liu, T. Jiang, J. Song, Q. Wu, H. Jiang, On hybrid electroosmotic kinetics for field-effect-reconfigurable nanoparticle trapping in a four-terminal spiral microelectrode array, Electrophoresis (2018).
[11] J.H.-S. Kim, A. Marafie, X.-Y. Jia, J.V. Zoval, M.J. Madou, Characterization of DNA hybridization kinetics in a microfluidic flow channel, Sens. Actuators B Chem. 113 (2006) 281–289.
[12] S. Xu, J. Zhan, B. Man, S. Jiang, W. Yue, S. Gao, C. Guo, H. Liu, Z. Li, J. Wang, Y. Zhou, Real-time reliable determination of binding kinetics of DNA hybridization using a multi-channel graphene biosensor, Nat. Commun. 8 (2017) 14902.
[13] J. Wang, M. Aki, D. Onoshima, K. Arinaga, N. Kaji, M. Tokeshi, S. Fujita, N. Yokoyama, Y. Baba, Microfluidic biosensor for the detection of DNA by fluorescence enhancement and the following streptavidin detection by fluorescence quenching, Biosens. Bioelectron. 51 (2014) 280–285.
[14] M. Cui, H. Feng, D. Guo, D. Wang, B. Zheng, A droplet-based microfluidic platform for kinetics-based detection of single nucleotide variation at room temperature with large discrimination factors, Sens. Actuators B Chem. 253 (2017) 731–737.
[15] K. Choi, A.H.C. Ng, R. Fobel, A.R. Wheeler, Digital microfluidics, Annu. Rev. Anal. Chem. 5 (2012) 413–440.
[16] J. Gao, X. Liu, T. Chen, P.-I. Mak, Y. Du, M.-I. Vai, B. Lin, R.P. Martins, An intelligent digital microfluidic system with fuzzy-enhanced feedback for multi-droplet manipulation, Lab Chip 13 (2013) 443–451.
[17] C. Li, K. Zhang, X. Wang, J. Zhang, H. Liu, J. Zhou, Feedback control system for large scale 2D digital microfluidic platforms, Sens. Actuators B Chem. 255 (2018) 3616–3622.
[18] J. Chang, J.J. Pak, Twin-plate electrowetting for efficient digital microfluidics, Sens. Actuators B Chem. 160 (2011) 1581–1585.
[19] L. Malic, T. Veres, M. Tabrizian, Biochip functionalization using electrowetting-on-dielectric digital microfluidics for surface plasmon resonance imaging detection of DNA hybridization, Biosens. Bioelectron. 24 (2009) 2218–2224.
[20] L. Malic, T. Veres, M. Tabrizian, Nanostructured digital microfluidics for enhanced surface plasmon resonance imaging, Biosens. Bioelectron. 26 (2011) 2053–2059.
[21] S.-Y. Teh, R. Lin, L.-H. Hung, A.P. Lee, Droplet microfluidics, Lab Chip 8 (2008) 198–220.
[22] C.A. Cortes-Quiroz, A. Azarbadegan, M. Zangeneh, Effect of channel aspect ratio of

3-D T-mixer on flow patterns and convective mixing for a wide range of Reynolds number, Sens. Actuators B Chem. 239 (2017) 1153–1176.
[23] P. Paik, V.K. Pamula, R.B. Fair, Rapid droplet mixers for digital microfluidic systems, Lab Chip 3 (2003) 253–259.
[24] P. Paik, V.K. Pamula, M.G. Pollack, R.B. Fair, Electrowetting-based droplet mixers for microfluidic systems, Lab Chip 3 (2003) 28–33.
[25] H.-W. Lu, F. Bottausci, J.D. Fowler, A.L. Bertozzi, C. Meinhart, C.-J. "CJ" Kim, A study of EWOD-driven droplets by PIV investigation, Lab Chip 8 (2008) 456–461.
[26] K. Choi, A.H.C. Ng, R. Fobel, D.A. Chang-Yen, L.E. Yarnell, E.L. Pearson, C.M. Oleksak, A.T. Fischer, R.P. Luoma, J.M. Robinson, J. Audet, A.R. Wheeler, Automated digital microfluidic platform for magnetic-particle-based immunoassays with optimization by design of experiments, Anal. Chem. 85 (2013) 9638–9646.
[27] S. Kalsi, M. Valiadi, M.-N. Tsaloglou, L. Parry-Jones, A. Jacobs, R. Watson, C. Turner, R. Amos, B. Hadwen, J. Buse, C. Brown, M. Sutton, H. Morgan, Rapid and sensitive detection of antibiotic resistance on a programmable digital microfluidic platform, Lab Chip 15 (2015) 3065–3075.
[28] B. Seale, C. Lam, D.G. Rackus, M.D. Chamberlain, C. Liu, A.R. Wheeler, Digital microfluidics for immunoprecipitation, Anal. Chem. 88 (2016) 10223–10230.
[29] I. Barbulovic-Nad, H. Yang, P.S. Park, A.R. Wheeler, Digital microfluidics for cell-based assays, Lab Chip 8 (2008) 519–526.
[30] C. Dong, T. Chen, J. Gao, Y. Jia, P.I. Mak, M.I. Vai, R.P. Martins, On the droplet velocity and electrode lifetime of digital microfluidics: voltage actuation techniques and comparison, Microfluid. Nanofluidics 18 (2015) 673–683.
[31] E. Samiei, M.D. de Leon Derby, A. Van den Berg, M. Hoorfar, An electro-hydrodynamic technique for rapid mixing in stationary droplets on digital microfluidic platforms, Lab Chip 17 (2017) 227–234.
[32] P. García-Sánchez, A. Ramos, F. Mugele, Electrothermally driven flows in ac electrowetting, Phys. Rev. E 81 (2010) 015303.
[33] H. Dai, M. Meyer, S. Stepaniants, M. Ziman, S. Stoughton, Use of hybridization kinetics for differentiating specific from non-specific binding to oligonucleotide microarrays, Nucleic Acids Res. 30 (2002) 86e.
[34] C. Dong, Y. Jia, J. Gao, T. Chen, P.-I. Mak, M.-I. Vai, R.P. Martins, A 3D microblade structure for precise and parallel droplet splitting on digital microfluidic chips, Lab Chip 17 (2017) 896–904.
[35] D. Mampallil, H. Burak Eral, A. Staicu, F. Mugele, D. van den Ende, Electrowetting-driven oscillating drops sandwiched between two substrates, Phys. Rev. E 88 (2013) 053015.
[36] S.H. Ko, H. Lee, K.H. Kang, Hydrodynamic Flows in Electrowetting, Langmuir 24 (2008) 1094–1101.
[37] H. Lee, S. Yun, S.H. Ko, K.H. Kang, An electrohydrodynamic flow in ac electrowetting, Biomicrofluidics 3 (2009) 044113.
[38] W. Liu, Y. Ren, Y. Tao, B. Yao, Y. Li, Simulation analysis of rectifying microfluidic mixing with field-effect-tunable electrothermal induced flow, Electrophoresis 39 (2018) 779–793.
[39] W. Liu, Y. Ren, Y. Tao, X. Chen, Q. Wu, Electrode Cooling Effect on Out-Of-Phase Electrothermal Streaming in Rotating Electric Fields, Micromachines 8 (2017) 327.
[40] W. Liu, Y. Ren, J. Shao, H. Jiang, Y. Ding, A theoretical and numerical investigation of travelling wave induction microfluidic pumping in a temperature gradient, J. Phys. D Appl. Phys. 47 (2014) 075501.
[41] Y. Li, Y. Ren, W. Liu, X. Chen, Y. Tao, H. Jiang, On controlling the flow behavior driven by induction electrohydrodynamics in microfluidic channels, Electrophoresis 38 (2017) 983–995.
[42] M. Dusselier, P. Van Wouwe, A. Dewaele, P.A. Jacobs, B.F. Sels, Shape-selective zeolite catalysis for bioplastics production, Science 349 (2015) 78–80.
[43] A. Nagaki, M. Togai, S. Suga, N. Aoki, K. Mae, J. Yoshida, Control of extremely fast competitive consecutive reactions using micromixing. selective friedel − crafts aminoalkylation, J. Am. Chem. Soc. 127 (2005) 11666–11675.
[44] S.C.B. Selvamony, Kinetics and product selectivity (Yield) of second order competitive consecutive reactions in fed-batch reactor and plug flow reactor, ISRN Chem. Eng. (2013) (2013) 1–17.
[45] H.J. Pandya, K. Dhingra, D. Prabhakar, V. Chandrasekar, S.K. Natarajan, A.S. Vasan, A. Kulkarni, H. Shafiee, A microfluidic platform for drug screening in a 3D cancer microenvironment, Biosens. Bioelectron. 94 (2017) 632–642.
[46] P.T. Kumar, F. Toffalini, D. Witters, S. Vermeir, F. Rolland, M.L.A.T.M. Hertog, B.M. Nicolaï, R. Puers, A. Geeraerd, J. Lammertyn, Digital microfluidic chip technology for water permeability measurements on single isolated plant protoplasts, Sens. Actuators B Chem. 199 (2014) 479–487.

Mingzhong Li is currently pursuing the Ph.D. degree with the Faculty of Science and Technology - ECE and State Key Laboratory of Analog and Mixed-Signal VLSI, University of Macau (China). His research interests focus on the technology development of digital microfluidic analysis systems and their applications in biochemistry.

Cheng Dong received the Ph.D. degree in electrical and computer engineering from the University of Macau, Macao, China, in 2017. He is currently a postdoctoral fellow with State Key Laboratory of Analog and Mixed-Signal VLSI, University of Macau. Since 2012, he has been involved in the research areas of electronic automation in the digital microfluidic system, software development, molecular biology for disease detection.

Man-Kay Law obtained his Ph.D. in 2011 from Hong Kong University of Science and Technology (Hong Kong). He is currently an associate professor in the State Key Laboratory of Analog and Mixed Signal VLSI, University of Macau, China. His research interests involve analog/sensing electronics for integrated and multidisciplinary areas.

Yanwei Jia received her Ph.D. from National University of Singapore in 2006. She is currently an assistant professor at the State Key Laboratory of Analog and Mixed Signal VLSI, University of Macau, Macau SAR, China. Her research interests include digital microfluidics development and its application in biomedical engineering, and point-of-care testing for disease diagnostics.

Pui-In Mak received the Ph.D. degree from University of Macau (UM), Macao, China, in 2006. He is currently Full Professor at UM Faculty of Science and Technology – ECE, and Associate Director (Research) at the UM State Key Laboratory of Analog and Mixed-Signal VLSI. His research interests are on analog and radio-frequency (RF) circuits and systems for wireless and multidisciplinary innovations.

Rui P. Martins received the Ph.D. degrees as well as the Habilitation for Full Professor in electrical engineering and computers from the Department of Electrical and Computer Engineering, Instituto Superior Técnico (IST), TU of Lisbon, Portugal, in 1992 and 2001, respectively. He is currently Chair Professor at the Department of Electrical and Computer Engineering, Faculty of Science and Technology, University of Macau (UM), as well as the Vice-Rector (Global Affairs) of UM. He is also the Founding Director of the Analog and Mixed-Signal VLSI Research Laboratory of UM (now elevated to the State Key Laboratory of China since 2011).